A Strong Dependence of the P-P Bond Length on the Transition Metal Component in $ThCr_2Si_2$-Type Phosphides CaM_2P_2 (M = Fe, Ni): The Influence of d Band Position and σ_p^* Mixing

Dae-Bok Kang

Department of Chemistry, Kyungsung University, Busan 608-736, Korea
Received April 18, 2003

An analysis of the bonding situation in CaM_2P_2 (M=Fe, Ni) with $ThCr_2Si_2$ structure is made in terms of DOS and COOP plots. The main contributions to covalent bonding are due to M-P and P-P interactions in both compounds. Particularly, the interlayer P-P bonding by variation in the transition metal is examined in more detail. It turns out that the shorter P-P bonds in $CaNi_2P_2$ form as a result of the decreasing electron delocalization into σ_p^* of P_2 due to the weaker bonding interaction between the metal d and σ_p^* as the metal d band is falling from Fe to Ni.

Key Words : Phosphide, $ThCr_2Si_2$ structure, Electronic structure

Introduction

The well-known $ThCr_2Si_2$-type structure[1] is the highest number of materials for any crystal structure because of its possibility to adapt to strongly different atomic sizes as well as to a wide range of electron counts. In these $ThCr_2Si_2$ compounds remarkable differences exist regarding the bonding situation. While in $SrFe_2P_2$, *e.g.*, the shortest P-P distance is 3.43 Å, the corresponding value for $CaFe_2P_2$ is 2.71 Å and only 2.30 Å for $CaNi_2P_2$.[2] The short distance in $CaNi_2P_2$ is characteristic of a full P-P single bond. The long contacts of 3.43 Å in $SrFe_2P_2$ imply essentially no bonding at all. Hoffmann and Zheng analyzed the underlying nature of the chemical bonding in $BaMn_2P_2$ with $ThCr_2Si_2$ structure by using the extended Hückel (EH) method.[3] They have suggested that the interlayer P-P bonding is promoted by a depletion of the filled P-P σ_p^* band when going from Fe to Ni compound as a general trend for the transition metal series. However, this σ_p^* band is high and empty in all these compounds, therefore it cannot be responsible for the trend in the P-P distances. In addition, the influence of M-P interaction on the P-P bonding was not taken into account in their paper.

In the present paper, we will describe the main features of different types of interactions, *i.e.*, the M-P, M-M, and P-P bonding, regarding the $ThCr_2Si_2$-type structure represented by the CaM_2P_2 (M=Fe, Ni) compounds with long and short P-P distances. In order to understand the striking difference of the interlayer P-P distances provided by variation in the transition metal, we present an analysis of the P-P bonding within the M-P interacting framework on the basis of EH tight-binding band calculations.[4,5] The calculations were performed by using the CAESAR package,[6] which provides useful graphical outputs such as band structure, density of states (DOS), and crystal orbital overlap population (COOP) curves. The atomic orbital parameters used for the calculations are given in Table 1. The theoretical tool we use is perturbation theory and its predictions are confirmed by actual molecular orbital calculations, as will be discussed later. Previous theoretical investigations of these compounds are scarce and confined to calculations using the Linearized Augmented Plane-Wave (LAPW) method.[7]

Table 1. Atomic Parameters Used in the Calculations

atom	orbital	H_{ii} (eV)	ζ_1	C_1^a	ζ_2	C_2^a	ref
Fe	4s	−7.6	1.90				10
	4p	−3.8	1.90				
	3d	−9.2	5.35	0.5366	1.80	0.6678	
Ni	4s	−8.1	2.10				11
	4p	−4.2	2.10				
	3d	−12.4	5.75	0.5325	2.00	0.6626	
P	3s	−18.6	1.75				10
	3p	−14.0	1.30				

[a]Coefficients in double-ζ expansion.

Crystal Structure

Figure 1 shows the tetragonal unit cell for $CaFe_2P_2$ (or $CaNi_2P_2$) with space group I4/mmm and cell parameters a = 3.855 (3.916) Å, c = 9.985 (9.363) Å. The structural parameters used for the present calculations are taken from ref. 2. The z axes are always parallel to the c axis of the unit cell. The structure consists of $M_2P_2^{2-}$ layers of MP_4 tetrahedra and Ca^{2+} layers, alternately stacked along the c axis. The $M_2P_2^{2-}$ layers contains the strong covalent M-P bonding that is suggested by the short distances comparable to the Pauling single bond radius sums (d_{Fe-P} = 2.27, d_{Ni-P} = 2.25 Å),[8] whereas the interlayer distances between the P atoms show a great variety of values. In Table 2 we list the P-P distances of some first and second row transition metal phosphides. They decrease strongly as the transition metal moves from the left

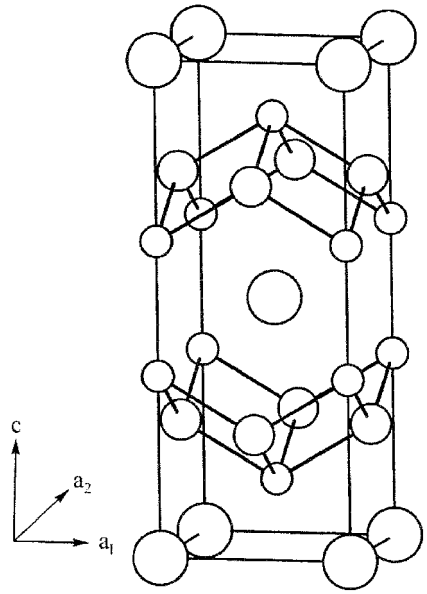

Figure 1. Unit cell of the tetragonal CaM_2P_2 (M=Fe, Ni) with $ThCr_2Si_2$ structure: large spheres, Ca; medium spheres, M (Fe or Ni); small spheres, P.

Table 2. Interlayer P-P Distances in Some $ThCr_2Si_2$-Type Phosphides[2,12]

compound	$d_{P\text{-}P}$ (Å)	compound	$d_{P\text{-}P}$ (Å)
$CaFe_2P_2$	2.710	$CaRu_2P_2$	2.576
$CaCo_2P_2$	2.454	$CaRh_2P_2$	2.255
$CaNi_2P_2$	2.297	$CaPd_2P_2$	2.166

to the right-hand side in the periodic table. An electronic effect governing the observed trend in the P-P distances will be explained in the following section.

Results and Discussion

Electronic structure of $CaFe_2P_2$. In this section we shall see how the electronic structure of the three-dimensional (3D) $Fe_2P_2^{2-}$ lattice evolves as we build the 3D solid by putting $Fe_2P_2^{2-}$ layers together. First, the interlayer P-P unit may be thought of as being formed by bringing together the P atoms from two layers. The P_2 sublattice of 3D $Fe_2P_2^{2-}$ will then be constructed from these units, and finally, the Fe atoms will be introduced into the lattice so that the P atoms can be positioned above and below the four-fold hollows of the Fe square sheet. The square lattice of Fe atoms in this structure is capped by P_2 units from both sides, with a P_2 axis perpendicular to the iron plane.

Crucial to our discussion will be the P_2 bonding unit, sometimes fully formed, sometimes not, in these $ThCr_2Si_2$-type structures. The molecular axis of P_2 orients parallel to the z direction of the cell, and the P-P distance within a P_2 unit is 2.71 Å. In order to understand the bonding relationships in $CaFe_2P_2$, we performed electronic structure calculations of representative molecular fragments and the

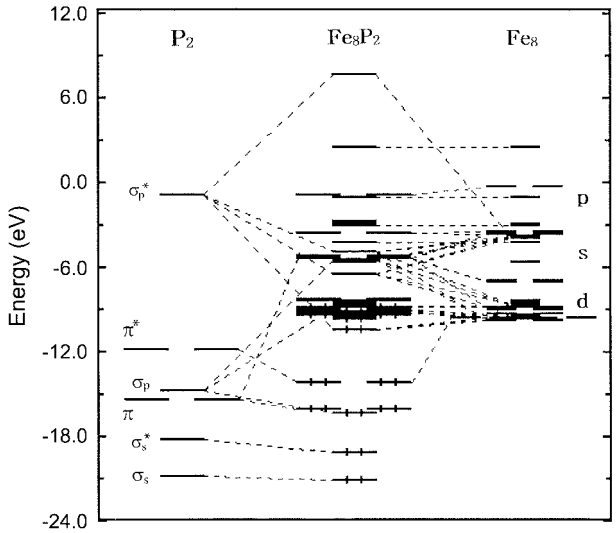

Figure 2. Orbital interaction diagram for an isolated molecular Fe_8P_2 cluster cut out of the solid.

complete 3D structure. We analyzed the electronic structure of basic building block Fe_8P_2 shown in **1** before studying the

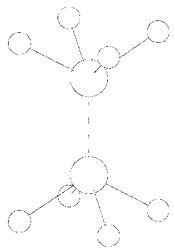

1

complete solid structure. The electronic structure of the P_2 unit is that of a typical homonuclear diatomic molecule. The energy levels of the diatomic orbitals are shown at the left side of Figure 2. What if iron atoms are added to the P_2 sublattice? The shortest Fe-P contact is 2.24 Å, a distance that is well within the iron-phosphorus bonding range. The Fe-P interactions are indeed quite strong, giving an overlap population (OP) of 0.46. The Fe-Fe interatomic distance within the square lattice is 2.73 Å. The schematic diagram in Figure 2 describes the interactions observed for the isolated molecular Fe_8P_2 cluster (**1**) cut out of the solid. The energy window of this diagram contains only the valence orbitals of the cluster. At low energy, both σ_p and π^* states of P_2 are stabilized by Fe 3d orbitals, mixed in a bonding fashion. The 3d(Fe)-π(P_2) interaction is relatively small, due to the large energy difference and small coupling overlap of the two, so that the majority of π states remain unchanged. At the highest energy level is primarily P_2 σ_p^*, antibonding to Fe 3d orbitals. The middle filled levels are slightly more complicated. They are represented by Fe 3d orbitals perturbed by P_2 σ_p and σ_p^*. Since σ_p and σ_p^* lie at respectively lower and higher energy than Fe 3d levels, P_2 σ_p^* mixes in a bonding way to Fe 3d orbitals while σ_p in an antibonding fashion. Electron density from the filled Fe 3d orbitals will be transferred to the empty P_2 σ_p^*.

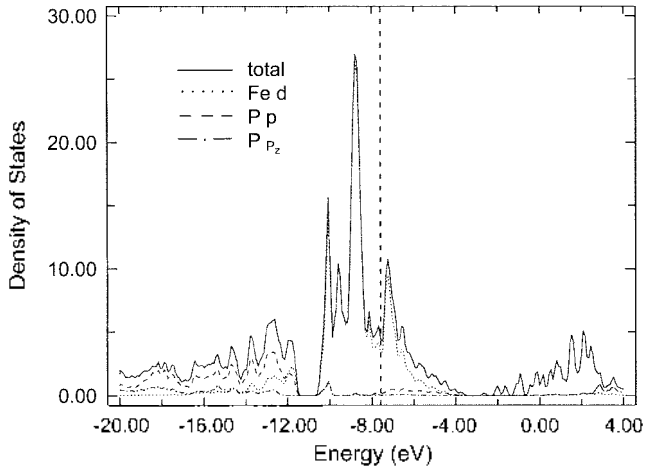

Figure 3. DOS plots for the 3D $(Fe_2P_2)^{2-}$ solid. Fermi energy is indicated with a vertical dashed line.

We next go on to the complete 3D solid. The electropositive element Ca can be considered as an electron donor; it formally transfers two electrons to the sublattice of $(Fe_2P_2)^{2-}$. Thus these atoms are presumed not to participate in covalent bonding and are not included in the calculations. Figure 3 displays the total DOS and its decomposition into Fe 3d and P 3p contributions calculated for the 3D $Fe_2P_2^{2-}$ structure. The shape of the DOS can easily be understood starting from the analysis of the orbitals of the cluster Fe_8P_2, which is the building blocks of this compound. First, the σ_p and π states of the P_2 dimer units appear in the interval −16 to −13 eV in the DOS. Their π^* states are associated with two peaks that lie around −12 eV. The bands with strong Fe 3d character are found between −10 and −7 eV. One should notice a P_2 σ_p^* bonding contribution to Fe 3d for the peak at −10 eV.

The average COOP curves for the bonding interactions present in the structure are plotted in Figure 4a. We can easily identify bonding contributions from the fragment molecular orbitals in Figure 2 and the DOS projections in Figure 3. As expected, the lower part of this energy region is mainly iron-phosphorus bonding. But now the two phosphorus atoms enter the interactions as a P_2 pair, whose orbitals are π, σ_p, π^*, and σ_p^*. The antibonding counterparts of 3d-π and 3d-π^* bonding orbitals lie above the Fermi level. The antibonding character between Fe 3d and σ_p is easily recognized from the peak at −9 eV that falls below the Fermi level. It is generated by the Fe-P antibonding interaction which increases the energy of a P-P σ_p bonding orbital and places it just below the Fermi level. There is a remarkable σ_p^* contribution at the bottom of the Fe 3d band. The orbital combination at −10 eV is apparently characterized by bonding interaction between the 3d and higher-lying empty σ_p^*. Substantial electron filling of σ_p^* by mixing with Fe 3d leads to weak interlayer P-P bonding (OP=0.58) in $CaFe_2P_2$.

The Fe-Fe distance in $CaFe_2P_2$ is 2.73 Å, much longer than that in Fe metal with 2.48 Å. The integrated COOP for the Fe-Fe bonds gives small positive values of 0.05, indicating no significant Fe-Fe bonding.

Influence of the transition metal. The substitution of the

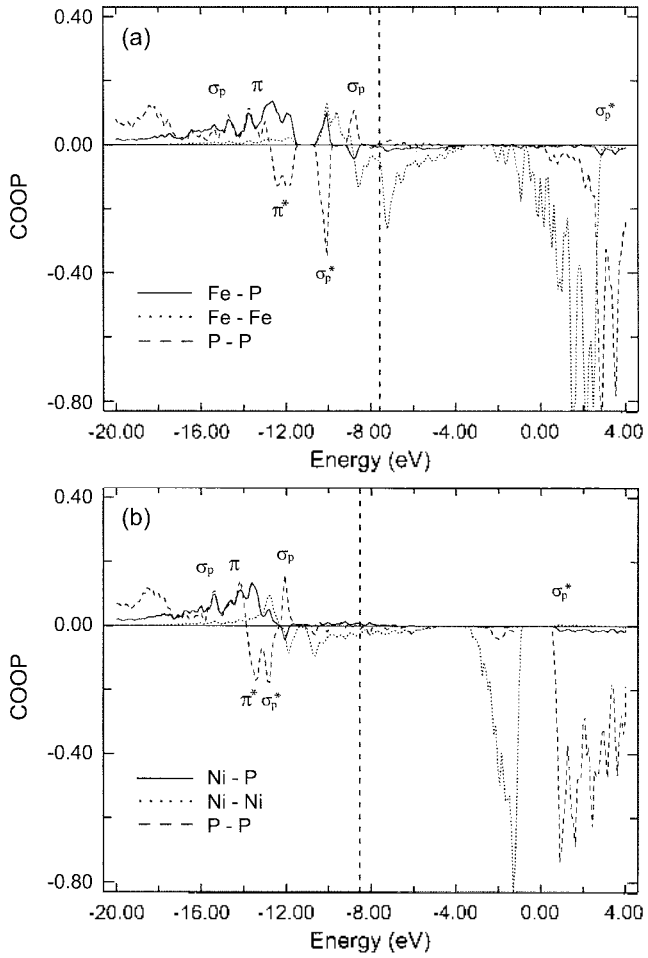

Figure 4. COOP plots for the M-P, M-M, and P-P bonds in the 3D $M_2P_2^{2-}$ solids: (a) $Fe_2P_2^{2-}$ and (b) $Ni_2P_2^{2-}$. Fermi energy is indicated with a vertical dashed line.

transition metal component (M=Fe) in $CaFe_2P_2$ by Ni leads to drastic changes of the P-P interlayer bonding and small increases (0.04 and 0.05 Å) in the M-M and M-P distances. The CaM_2P_2 compounds with M=Fe, Co, and Ni form P-P distances of 2.71, 2.45, and 2.30 Å, respectively (see Table 2). It appears that the transition metals from the left side of the periodic table tend to form longer P-P distances. To investigate the effects of transition metal substitution on the interlayer P-P bonding, we have calculated the band structures of $CaFe_2P_2$ and $CaNi_2P_2$. We substitute Fe in $CaFe_2P_2$ by Ni, keeping the geometry of the Fe compound in order to see only the electronic effect. The density of states for $CaNi_2P_2$ is essentially the same as for the iron compound, but the Fermi level is lower because the Ni d band comes down in energy. The P-P σ_p^* band lies so high that it is not occupied in all these compounds. If the interaction between the σ_p^* and the metal d bands is turned on, the weakening of interlayer P-P bonds will be favored by filling the σ_p^* antibonding states. Therefore, a distinctly stronger P-P bond for $CaNi_2P_2$ compared to $CaFe_2P_2$ cannot be due to the depopulation of the filled P-P σ_p^* states caused by the decreasing transition metal Fermi level.

What else will be the effects of different transition metals

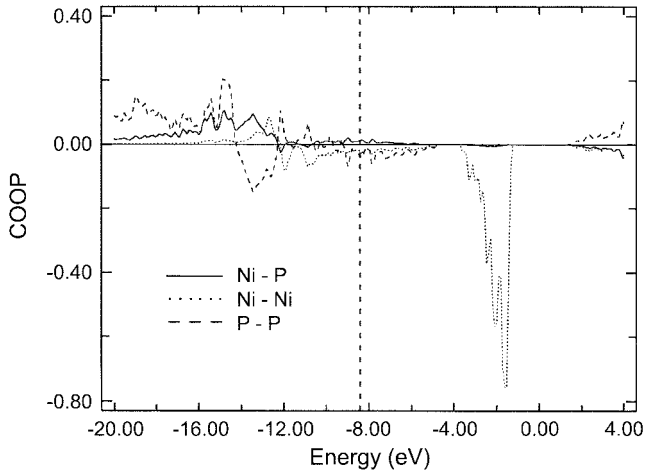

Figure 5. As in Figure 4b for the real $CaNi_2P_2$ structure. Fermi energy is indicated with a vertical dashed line.

on the interlayer P-P bonding in these compounds? This study attempts to answer this question. One such factor is the role of d band position. Let us analyze the observed trend in the P-P bonding as one moves from the iron to the nickel compound. The metal valence bands move down on the energy scale along that series. The σ_p orbital of P_2 is lower in energy than metal d band, but σ_p^* orbital energy lies well above it. As the d band goes down from Fe to Ni, there is progressively more and more interaction with σ_p, giving rise to stronger σ-donation to the metal. At the same time there is decreasing interaction between the d band and the σ_p^*. This decreases the d electron transfer into σ_p^* of P_2. Since the σ_p^* orbital is strongly antibonding, the decreased charge delocalization into P_2 σ_p^* increases the P-P bond order (OP=0.66) in $CaNi_2P_2$. The σ_p orbital is a nearly nonbonding type, so the σ-donation interaction is not very important for this context. Charge transfer from the metal to σ_p^* of P_2 is the key factor to explain the trend in P-P bond distances, and its change is expected from second order perturbation theory.[9] Figure 4b shows the calculated COOP curves for various bonding interactions in the $CaNi_2P_2$ structure obtained by replacing Fe in $CaFe_2P_2$ phase by Ni, as in Figure 4a. The solid lines are the average COOP of Ni-P bonds, the dashed lines of P-P bonds. Among the CaM_2P_2 compounds the general features of the COOP curves are all quite similar. Changes in the metal d band positions can mostly be attributed to changes in the d orbital energy of the constituent metal atoms. Substituting nickel for iron causes the bottom of the metal d band to shift to lower energy by approximately 3 eV. It should be noted that the antibonding region of interlayer P-P bond at −12.5 eV in Figure 4b decreases (compare it with the corresponding one at −10 eV in Figure 4a) when the d orbital energy is falling from Fe to Ni. This is because the filled Ni d-P_2 σ_p^* bonding component has less σ_p^* (or more metal d) character due to the decreased σ_p^* mixing. On the contrary, the rapid increase in P-P bond distances on going from the Ni to the Fe compound is due to stronger metal donation and participation of the P_2 σ_p^* orbital. Formally empty σ_p^* orbital interacts more strongly with the Fe d band, and its bonding component is occupied to a greater extent. Thus more population of electrons in σ_p^* weakens the P-P bonding in the Fe compound significantly. The more the σ_p^* is occupied, the weaker the P-P bonding and the longer the P-P bond. The P-P overlap populations are 0.58 and 0.66 in $CaFe_2P_2$ and $CaNi_2P_2$, respectively.

The metal-phosphorus and metal-metal interactions are slightly stronger in the iron compound mainly due to less occupation of their antibonding states. This is in agreement with the experimental observation[2] that the *a*-lattice constants for the Fe compound are slightly shorter compared with the Ni compound. For the real $CaNi_2P_2$ structure, COOP curves of Ni-P, Ni-Ni, and P-P bonds are plotted in Figure 5. This is analogous to what happened in Figure 4b. The σ_p^* + metal antibonding states are not shown in the figure because its states with short P-P bonds appear at very high energy of 10 eV.

Conclusions

In summary, the interlayer P-P bonding in $CaFe_2P_2$ and $CaNi_2P_2$ with $ThCr_2Si_2$ structure is controlled by the transition metal d band position, but in a way different from previous findings[3]. We do not find the bond formation by the depopulation of filled P-P σ_p^* orbital when going from Fe to Ni compound. Shorter P-P bonds in the Ni compound are derived from less population of P-P σ_p^* antibonding states due to the decreasing σ_p^* mixing with the lowered d band. This effect is working toward shorter P-P bonds on going from left to right in the transition series. If the M_2P_2 (M=transition element) layers are well separated from each other due to large atoms like Ba or La, it should be not possible to form a short P-P contact by geometric reasons. In any event, it is not resonable to separate the P-P bond from the metal-phosphorus interaction.

Acknowledgment. This work was supported by Kyungsung University Research Grant in 2003.

References

1. Ban, Z.; Sikirica, M. *Acta Crystallogr.* **1965**, *18*, 594.
2. Mewis, A. *Z. Naturforsch.* **1980**, *B35*, 141.
3. Hoffmann, R.; Zheng, C. *J. Phys. Chem.* **1985**, *89*, 4175.
4. Whangbo, M.-H.; Hoffmann, R. *J. Am. Chem. Soc.* **1978**, *100*, 6093.
5. Hoffmann, R. *Solids and Surfaces: A Chemist's View of Bonding in Extended Structures*; VCH Publishers: New York, 1988.
6. Ren, J.; Liang, W.; Whangbo, M.-H. *Crystal and Electronic Structure Analysis Using CAESAR*; http://www.PrimeC.com, 1998.
7. Gustenau, E.; Herzig, P.; Neckel, A. *J. Solid State Chem.* **1997**, *129*, 147.
8. Pauling, L. *The Nature of the Chemical Bond*; Cornell Press: New York, 1960.
9. Hoffmann, R. *Acc. Chem. Res.* **1971**, *4*, 1.
10. Alvarez, S. *Tables of Parameters for Extended Hückel Calculations*; Barcelona, Spain, 1995.
11. Vela, A.; Gazquez, J. L. *J. Phys. Chem.* **1988**, *92*, 5688.
12. Johrendt, D.; Felser, C.; Jepsen, O.; Anderson, O. K.; Mewis, A.; Rouxel, J. *J. Solid State Chem.* **1997**, *130*, 254.